Antiviral Research 161 (2019) 70–84

Contents lists available at ScienceDirect

Antiviral Research

journal homepage: www.elsevier.com/locate/antiviral

Encephalomyocarditis virus 2C protein antagonizes interferon-β signaling pathway through interaction with MDA5

Liang Li[a], Hui Fan[a], Zhongbao Song[a], Xuewei Liu[a], Juan Bai[a,b,*], Ping Jiang[a]

[a] Key Laboratory of Animal Diseases Diagnostic and Immunology, Ministry of Agriculture, MOE International Joint Collaborative Research Laboratory for Animal Health & Food Safety, College of Veterinary Medicine, Nanjing Agricultural University, Nanjing 210095, China

[a] Jiangsu Co-innovation Center for Prevention and Control of Important Animal Infectious Diseases and Zoonoses, Yangzhou, China

ARTICLE INFO

Keywords:
EMCV
IFN-β inhibition
MDA5
Non-structural protein 2C

ABSTRACT

Encephalomyocarditis virus (EMCV) is one of the most important picornavirus. It infects many mammalian species and causes encephalitis, myocarditis, neurologic diseases, diabetes and reproductive disorders in pigs. And it evolves mechanisms for escaping innate immune responses. But the viral pathogenesis has not been understood completely. In this study, we firstly found that EMCV protein 2C is a strong IFN-β antagonist that interacts with MDA5 to inhibit induction of the IFN-β signal pathway. The mutations in amino acid residue V26 of 2C decrease the inhibition of IFN-β promoter activity and lost the ability to interact with MDA5, compared with wild type 2C protein. The rescued viruses with mutations in 2C (rV26A and rK25-3A) induced significantly higher IFN-β mRNA and protein levels in PK-15, HEK-293A and N2a cells, compared to wild type EMCV and the repaired viruses rV26A(R) and rK25-3A(R). These data indicate that the amino acid residue V26 of EMCV 2C plays important roles in inhibiting type I IFN production by interacting with MDA5.

1. Introduction

Encephalomyocarditis virus (EMCV) is a non-enveloped single-stranded RNA virus belonging to the genus *Cardiovirus* in the *Picornaviridae* family. It is a research model for viral myocarditis and diabetes. It infects many mammalian species, causing pathologies such as encephalitis, myocarditis, neurologic diseases, diabetes and reproductive disorders (Carocci and Bakkali-Kassimi, 2012). EMCV has one open reading frame that encodes a single polyprotein that is cleaved by 3C protease to produce four capsid proteins and eight non-structural proteins (Loughran et al., 2011). The non-structural proteins are responsible for genome replication and assembly. Two proteins of EMCV are known to regulate the host innate immune response. EMCV 3C disrupts the TANK–TBK1–IKKε–IRF3 complex, thereby attenuating type I interferon production (Huang et al., 2017). The 2B protein of EMCV activates the NLRP3 inflammasome (Ito et al., 2012). We hypothesized that other proteins of EMCV may also regulate the innate immune system.

The 36.5 kDa EMCV 2C protein is 325 amino acids in length and contains an ATPase domain and a putative helicase domain (Carocci and Bakkali-Kassimi, 2012). Bioinformatics analysis suggests that the ATPase activity of 2C is essential for virus replication (Hindiyeh et al., 1999). 2C protein may activate ER stress molecules involved in EMCV-induced autophagy (Hou et al., 2014), and may also interact with membranes and help determine the specificity of encapsidation for newly synthesized viral RNA (Banerjee et al., 2001). The 2C protein in other picornaviruses induces formation of membrane vesicles, binds to the 3′-UTR of viral genome and is involved in viral genome replication. However, it is not known whether EMCV 2C is also involved in the regulation of the innate immune response.

Type I interferon, containing IFN-α and IFN-β, is critical for innate immunity, and is required to activate adaptive immunity (Garcia-Sastre and Biron, 2006a; Takaoka and Yanai, 2006). A battery of pattern recognition receptors, such as the retinoic acid-inducible gene-I (RIG-I)-like receptors (RLRs) and the toll-like receptors (TLRs), recognize pathogen-associated molecular patterns (PAMPs) (Akira et al., 2006; Medzhitov and Janeway, 2002; Stetson and Medzhitov, 2006). Cytosolic RLRs, such as RIG-I and MDA5, can recognize RNA viruses, while TLRs are localized in endosomes or at the cell surface (Akira et al., 2006; Medzhitov and Janeway, 2002; Stetson and Medzhitov, 2006). RLRs contain three conserved domains. The N terminus includes caspase recruitment domains (CARDs) and a DExD/H box helicase domain, while the C-terminus contains a regulatory/repression domain.

Upon recognizing a viral infection, RIG-I and MDA5 are activated

* Corresponding author. Key Laboratory of Animal Diseases Diagnostic and Immunology, Ministry of Agriculture, MOE International Joint Collaborative Research Laboratory for Animal Health & Food Safety, College of Veterinary Medicine, Nanjing Agricultural University, Nanjing 210095, China.
E-mail address: baijuan@njau.edu.cn (J. Bai).

https://doi.org/10.1016/j.antiviral.2018.10.010
Received 6 August 2018; Received in revised form 30 September 2018; Accepted 8 October 2018
Available online 10 October 2018

Table 1
Primers used to generate individual viral protein-expressing plasmids, 2C mutants and the IFN-β signaling pathway protein-expressing plasmids.

Primer	Sequence (5′→3′)[a]
eGFP-F(*EcoR* I)	CGC**GAATTC**ATGGTGAGCAAGGGC
eGFP-Flag-R(*Xho* I)	GCG**CTCGAG**TCACTTATCGTCGTCATCCTTGTAATCCTTGTACAGCTCGTC
L-eGFP-F(*EcoR* I)	CGC**GAATTC**ATGGCCACAACTATGGA
L-eGFP-linker-R	GCTCCTCGCCCTTGCTCACCATAGATCCCTGTAACTCGAAAACG
L-eGFP-linker-F	CGTTTTCGAGTTACAGGGATCTATGGTGAGCAAGGGCGAGGAGC
L-eGFP-Flag(*Xho* I)	GCG**CTCGAG**TCACTTATCGTCGTCATCCTTGTAATCCTTGTACAGCTCGTC
2A-F(*EcoR* I)	CGC**GAATTC**ATGAGTCCAAATGCCCTA
2A-Flag-R(*Xho* I)	GCG**CTCGAG**TCACTTATCGTCGTCATCCTTGTAATCCCCTGGATTTGTCTCAA
2B-F(*EcoR* I)	CGC**GAATTC**ATGCCCTTCATGTTTAGA
2B-Flag-R(*Xho* I)	GCG**CTCGAG**TCACTTATCGTCGTCATCCTTGTAATCTTGTTGTTGGAAAAGAGA
2C-F(*EcoR* I)	CGC**GAATTC**ATGTCCCCCTTGAAAC
2C-Flag-R(*Xho* I)	GCG**CTCGAG**TCACTTATCGTCGTCATCCTTGTAATCTTGTGCCACAAGGGT
3A-F(*EcoR* I)	CGC**GAATTC**ATGGCTCCAGTAGAC
3A-Flag-R(*Xho* I)	GCG**CTCGAG**TCACTTATCGTCGTCATCCTTGTAATCCTGCTCCTGCTCATC
3C-F(*EcoR* I)	CGC**GAATTC**ATGGGACCAAACCCTGT
3C-Flag-R(*Xho* I)	GCG**CTCGAG**TCACTTATCGTCGTCATCCTTGTAATCCTGTGGCTCAAAGGCA
3D-F(*EcoR* I)	ATA**GAATTC**ATGGGTGCTCTCGAGAGA
3D-Flag-R(*Kpn* I)	CGC**GGTACC**TCACTTATCGTCGTCATCCTTGTAATCCCAGAACAGACTCCTCC
2C(1-188)-F(*EcoR* I)	CGC**GAATTC**ATGTCCCCCTTGAAAC
2C(1-188)-Flag-R(*Xho* I)	GCG**CTCGAG**TCACTTATCGTCGTCATCCTTGTAATCAGTCGAAACCATCT
2C(10-325)-F(*EcoR* I)	CGC**GAATTC**ATGTTCTCCCTAGCCA
2C(10-325)-Flag-R(*Xho* I)	GCG**CTCGAG**TCACTTATCGTCGTCATCCTTGTAATCTTGTGCCACAAGGGT
2C(15-325)-F(*EcoR* I)	CGC**GAATTC**ATGAACCTGGACTGGG
2C(15-325)-Flag-R(*Xho* I)	GCG**CTCGAG**TCACTTATCGTCGTCATCCTTGTAATCTTGTGCCACAAGGGT
2C(20-325)-F(*EcoR* I)	CGC**GAATTC**ATGGTCAAGACTGTGG
2C(20-325)-Flag-R(*Xho* I)	GCG**CTCGAG**TCACTTATCGTCGTCATCCTTGTAATCTTGTGCCACAAGGGT
2C(25-325)-F(*EcoR* I)	CGC**GAATTC**ATGAAGGTGGTTG
2C(25-325)-Flag-R(*Xho* I)	GCG**CTCGAG**TCACTTATCGTCGTCATCCTTGTAATCTTGTGCCACAAGGGT
2C(28-325)-F(*EcoR* I)	CGC**GAATTC**ATGGATTGGTTTG
2C(28-325)-Flag-R(*Xho* I)	GCG**CTCGAG**TCACTTATCGTCGTCATCCTTGTAATCTTGTGCCACAAGGGT
2C(31-325)-F(*EcoR* I)	CGC**GAATTC**ATGGGGACATGGATAG
2C(31-325)-Flag-R(*Xho* I)	GCG**CTCGAG**TCACTTATCGTCGTCATCCTTGTAATCTTGTGCCACAAGGGT
2C(63-325)-F(*EcoR* I)	CGC**GAATTC**ATGGGAATGGCCGCCTA
2C(63-325)-Flag-R(*Xho* I)	GCG**CTCGAG**TCACTTATCGTCGTCATCCTTGTAATCTTGTGCCACAAGGGT
2C(97-325)-F(*EcoR* I)	CGC**GAATTC**ATGGAAAAATTCAGAC
2C(97-325)-Flag-R(*Xho* I)	GCG**CTCGAG**TCACTTATCGTCGTCATCCTTGTAATCTTGTGCCACAAGGGT
2C(133-325)-F(*EcoR* I)	CGC**GAATTC**ATGGTTATTGCCCAGG
2C(133-325)-Flag-R(*Xho* I)	GCG**CTCGAG**TCACTTATCGTCGTCATCCTTGTAATCTTGTGCCACAAGGGT
2C(K25A)-F	GTCAAGACTGTGGAA**GCG**GTGGTTGATTGGTTT
2C(K25A)-R	AAACCAATCAACCAC**CGC**TTCCACAGTCTTGAC
2C(V26A)-F	AAGACTGTGGAAAAG**GCG**GTTGATTGGTTTGGG
2C(V26A)-R	CCCAAACCAATCAAC**CGC**CTTTTCCACAGTCTT
2C(V27A)-F	ACTGTGGAAAAGGTG**GCT**GATTGGTTTGGGACA
2C(V27A)-R	TGTCCCAAACCAATC**AGC**CACCTTTTCCACAGT
2C(K25-3A)-F	GTCAAGACTGTGGAA**GCGGCGGCT**GATTGGTTTGGGACA
2C(K25-3A)-R	TGTCCCAAACCAATC**AGCCGCCGC**TTCCACAGTCTTGAC
MDA5-F(*Kpn* I)	GCC**GGTACC**ATGTCGAATGGGTATTC
MDA5-HA-R(*Xho* I)	GCG**CTCGAG**TCAAGCGTAGTCTGGGACGTCGTATGGGTAATCCTCATCACTAAATA
RIGI-F(*Kpn* I)	ATA**GGTACC**ATGACCACCGAGCAGCGA
RIGI-HA-R(*Xho* I)	GCG**CTCGAG**TCAAGCGTAGTCTGGGACGTCGTATGGGTATTTGGACATTTCTGCTG
MAVS-F(*Kpn* I)	GCC**GGTACC**ATGCCGTTTGCTGAAGA
MAVS-HA-R(*Xho* I)	TAT**CTCGAG**TCAAGCGTAGTCTGGGACGTCGTATGGGTAGTGCAGACGCCGCCGG
IRF3-F(*EcoR* I)	CGC**GAATTC**ATGGGAACCCCAAAGC
IRF3-HA-R(*Xho* I)	TAT**CTCGAG**TCAAGCGTAGTCTGGGACGTCGTATGGGTAGCTCTCCCCAGGGCC
P65-F(*Kpn* I)	ATA**GGTACC**ATGGACGAACTGT
P65-HA-R(*Xho* I)	TAT**CTCGAG**TCAAGCGTAGTCTGGGACGTCGTATGGGTAGGGAGCTGATCTGACT
IKKβ-F(*BamH* I)	CGC**GAATTC**ATGACTTACCGATATCAT
IKKβ-HA-R(*Xho* I)	TAT**CTCGAG**TCAAGCGTAGTCTGGGACGTCGTATGGGTAGTGATAGGATACTAGCT

[a] The genomic positions of the primers were based on the sequence under GenBank accession number HM641897. The restriction enzyme sites used for cloning and locations of mutations are indicated are in bold. The C-terminal Flag or HA tag sequence in the "R" primers are underlined.

and interact with the CARD of the mitochondrial adaptor protein MAVS (also known as VISA, CARDIF or IPS-1). Activated MAVS interacts with and activates the transcription factors IFN regulatory factor 3 (IRF3) and nuclear factor-κB (NF-κB) (Fitzgerald et al., 2014; Kang et al., 2002; Yoneyama et al., 2004). The activated transcription factors enter the nucleus and stimulate the expression of type I IFNs and inflammatory cytokines (Glatt et al., 2017; Sato et al., 1998; Yoneyama et al., 1998). Subsequently, type I IFNs bind to their cell surface receptors, activating the JAK and STAT signaling pathways and increasing the expression of interferon-stimulated genes (ISGs) such as ISG 15, ISG 56, OAS and Mxs (Darnell, 1998; Vlotides et al., 2004; Zhao et al., 2016). RIG-I and MDA5 therefore play important roles in activation of the IFN signaling pathway. A previous study determined that MDA5, but not RIG-I, is activated by EMCV (Takeuchi and Akira, 2008). Nevertheless, whether EMCV regulates the innate immune response is not known.

Many RNA viruses, such as coxsackievirus A6, and A16, and

Table 2
Primers used for RT-PCR.

Primer	Sequence (5′→3′)
hMDA5-F	GCTGAAGTAGGAGTCAAAGCCC
hMDA5-R	CCACTGTGGTAGCGATAAGCAG
hRIG-I-F	CACCTCAGTTGCTGATGAAGGC
hRIG-I-R	GTCAGAAGGAAGCACTTGCTACC
hIFN-β-F	CGCCGCATTGACCATCTA
hIFN-β-R	GACATTAGCCAGGAGGTTCTCA
hISG56-F	GCCTTGCTGAAGTGTGGAGGAA
hISG56-R	ATCCAGGCGATAGGCAGAGATC
hISG15-F	GACAAATGCGACGAACCTC
hISG15-R	CCGCTCACTTGCTGCTT
hMX1-F	CCATCGGAATCTTGACG
hMX1-R	GCTTCGGACAGGCTCAG
hOAS-F	CTCAAGAGCCTCATCCGC
hOAS-R	GACCGTCCGAAATCCCT
hGAPDH-F	GAGTCAACGGATTTGGTCGT
hGAPDH-R	GACAAGCTTCCCGTTCTCAG
pIFN-β-F	GGCTGGAATGAAACCGTCAT
pIFN-β-R	TCCAGGATTGTCTCCAGGTCA
pISG56-F	AAATGAATGAAGCCCTGGAGTATT
pISG56-R	AGGGATCAAGTCCACAGATTTT
pISG15-F	GGTGCAAAGCTTCAGAGACC
pISG15-R	GTCAGCCAGACCTCATAGGC
pMX1-F	CATCTGTAAAACTCTGCCCCTGT
pMX1-R	CATCTTCCCGCTTTCATCCT
pOAS-F	GGGACCTAGACAAGTTCATCG
pOAS-R	ATGGCTTCCTTGACCTGTG
pGAPDH-F	ACATGGCCTCCAAGGAGTAAGA
pGAPDH-R	GATCGAGTTGGGGCTGTGACT
mIFN-β-F	ATGAGTGGTGGTTGCAGGC
mIFN-β-R	TGACCTTTCAAATGCAGTAGATTCA
mISG56-F	TTTCAAGTCCCTTCCGCTAC
mISG56-R	GTACTCAGGGTTTTCTGGCTC
mISG15-F	GGTCTTACCCTTTCCAGTCTG
mISG15-R	CCCTTTCGTTCCTCACCAG
mMX1-F	ACCAGGGTGGCTGTAGG
mMX1-R	CAGGTTCCGCATCACAT
mOAS-F	ATGCTTTAAGTACAGGGACGG
mOAS-R	AGAGATACTTCGTTGGCACTG
mβ-Actin-F	CCACACCCGCCACCAGTTCG
mβ-Actin-R	TACAGCCCGGGGAGCATCGT

h means Human beings, p means Pigs and m means Mouse.

Table 3
Primers used for construction of an infectious cDNA clone of strain NJ08 mutants.

Primer	Sequence (5′→3′)[a]
B1-F(*Nhe*I)	ATT**GCTAGCT**GATCAAAATACA
B1-R(*Sac*I)	TCCAGG**GAGCTC**TAGAGTCCA
B2-F(*Nhe*I,*Sac*I)	ATT**GCTAGC**TTTTTTT**GAGCTC**CCTGGAATCCTTGGAAGAA
B2-R(*Xho*I)	TCT**CTCGAG**IDAGCACCCTGTGGCTCAAAG
B2m(V26A)-F	CCCAAACCAATCAAC**CGC**CTTTTCCACAGTCTT
B2m(V26A)-R	CCCAAACCAATCAAC**CGC**CTTTTCCACAGTCTT
B2m(K25-3A)-F	GTCAAGACTGTGGAA**GCGGCGGCT**GATTGGTTTGGGACA
B2m(K25-3A)-R	TGTCCCAAACCAATC**AGCCGCCGC**TTCCACAGTCTTGAC

[a] The genomic positions of the primers were based on the sequence under GenBank accession number HM641897. The restriction enzyme sites used for cloning and locations of mutations are shown in bold.

enterovirus D68 and 71, infect mammalian cells and suppress the type I IFN response (Takeuchi and Akira, 2008). EMCV infection inhibits the innate immune response in HEK293T cells (Huang et al., 2017), however, the mechanism by which EMCV does this has not been clarified. In this study, we found that EMCV can antagonize Type I IFNs in PK-15, HEK-293A, and N2a cells. We also showed that EMCV 2C inhibits poly (I:C)-mediated IFN-β promoter activity in HEK-293A cells, and interacts with MDA5, indicating that 2C may compromise MDA5 and prevent it from activating the IFN-β signaling pathway. Finally, we determined that amino acid V26 of the EMCV 2C protein plays a crucial role in regulating type I IFN expression. Together, the results reveal that EMCV uses a novel evasion mechanism to antagonize host innate immune responses.

2. Materials and methods

2.1. Cells, viruses and reagents

PK-15, HEK-293A, N2a, and BHK-21 cells were cultured in Dulbecco's modified Eagle's medium (Invitrogen, USA) at 37 °C in a humidified 5% CO2 atmosphere. DMEM was supplemented with 10% heat-inactivated fetal bovine serum (Gibco, USA), penicillin (250 U/mL), and streptomycin (250 μg/ml).

EMCV isolate NJ08 (GenBank accession no. HM641897) was passaged in BHK-21 cells. Recombinant viruses rNJ08/wt, rV26A, rV26A(R), rK25-3A, and rK25-3A(R) were derived from the infectious clone pCMV-rNJ08 [constructed in our laboratory as described previously (Fang et al., 2015)] and propagated in BHK-21. EMCV isolate NJ08 was inactivated by exposure to short-wave UV light (254 nm) for 1 h for use as a control.

Anti-Flag and anti-HA antibodies were purchased from Abmart, China, Rabbit anti-IRF3 polyclonal antibodies and anti-phosphorylated IRF3 antibodies and anti-β-actin from Santa Cruz Biotechnology, USA, a monoclonal antibody (MAb) for VP1 from our own laboratory, horseradish peroxidase-labeled goat anti-mouse antibody from Beyotime Biotechnology, China. poly (I:C) was purchased from Sigma–Aldrich U.S.A.

2.2. Plasmid construction

Genes encoding EMCV L, 2A, 2B, 2C, 3A, 3C, and 3D were amplified from pCMV-rNJ08. The PCR fragments were digested with restriction enzymes and cloned into a pCAGGS vector that had been modified to contain a 3′ FLAG-tag. Similarly, genes encoding MDA5, RIG-I, MAVS, IRF3, P65, and IKKβ were amplified from HEK293A cell genomic cDNAs and cloned using pCAGGS that had been modified to contain a 3′ HA-tag. The pGL3-IFN-β-Luc, pGL3-Basic, and pRL-TK vectors were purchased from Promega.

Truncated versions of the 2C protein, generated from pCAGGS-2C by PCR, were cloned into the pCAGGS vector using *Eco*R I and *Xho*I. The clones were designated pCAGGS-2C(1-188), (10-325), (15-325), (20-325), (25-325), (28-325), (31-325), (10-325), (63-325), (97-325), and (133-325). Site-directed mutagenesis was used to construct variants of the 2C protein containing single or multiple amino acid substitutions (V25A, V26A, V27A, and K25-3A). Constructs were validated by DNA sequencing. Primers are shown in Table 1.

2.3. Luciferase reporter assay

HEK-293A cells in 24-well plates were transfected with plasmid constructs, along with pIFN-β-luc or pGL3 (negative control), and 100 ng of pRL-TK. 24 h after transfection, cells were either mock-transfected or transfected with 1 μg/ml poly (I:C) using Lipofectamine® 3000 for 12 h. Cells were lysed in passive lysis buffer (Promega) and the activities of Firefly and *Renilla* luciferase were determined using the Dual-Luciferase Reporter 1000 Assay System (Promega), following the manufacturer's instructions. Results are expressed as fold changes of luciferase activities relative to measurements in mock-treated cells. All data are presented as means ± standard deviation (SD) for three independent experiments.

2.4. Co-immunoprecipitation and western blotting

HEK-293A cells were lysed in buffer containing 20 mM Tris-HCl pH 7.4–7.5, 150 mM NaCl, 1% NP-40, 1 mM EDTA, 5 mM $MgCl_2$, 10%

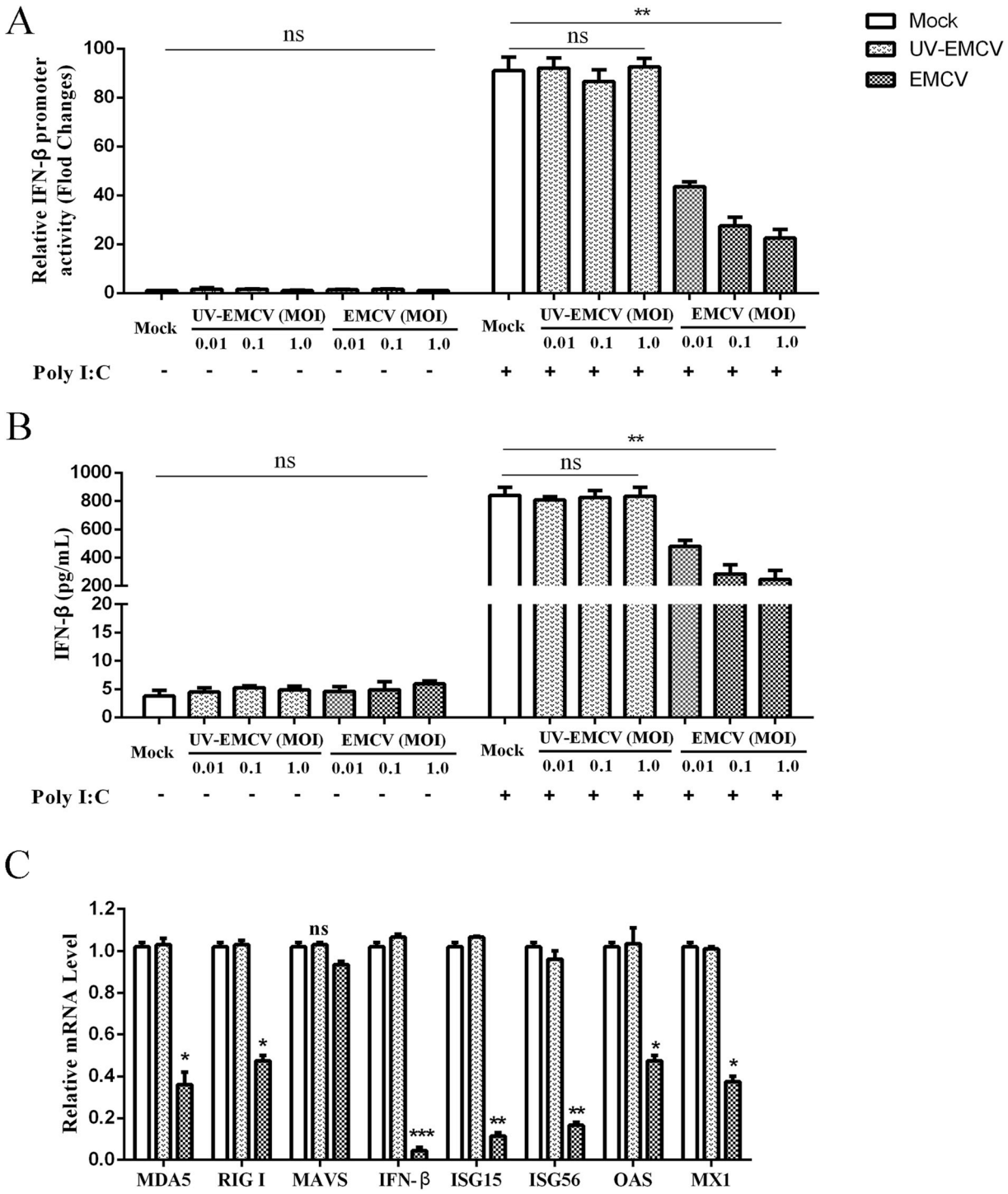

Fig. 1. EMCV infection suppresses poly (I:C)-mediated type I IFN signaling. (A) HEK-293A (2×10^5) cells were transfected with 400 ng of pIFN-β-luc plasmid and 10 ng of pRL-TK plasmid. At 24 hpt, the cells were inoculated with live or UV-inactivated EMCV NJ08 strain at an MOI of 0.01, 0.1 and 1, respectively. At 3 hpi, the cells were stimulated or unstimulated with poly (I:C) for 12 h and luciferase assays were performed. (B) HEK-293A (2×10^5) cells were inoculated with live or UV-inactivated EMCV NJ08 at an MOI of 0.01, 0.1 and 1, and transfected with poly (I:C). The culture supernatants were collected, and IFN-β protein levels were determined by ELISA. (C) HEK-293A cells were inoculated with live or UV-inactivated EMCV at an MOI of 0.1, followed by transfection with poly (I:C) for 12 h. The mRNA levels of MDA5, RIG I, MAVS, IFN-β, ISG15, ISG56, OAS, and MX1 were measured by real-time RT-PCR. Values are presented as mean ± SD for three independent experiments.

glycerol, and 1 mM PMSF. For co-immunoprecipitation (Co-IP), 1 ml of whole cell lysate was incubated with 1 μg of homograft mouse antibody and 20 μl of protein A/G agarose beads (Beyotime, China) at 4 °C for 2 h. The lysates were centrifuged (2500 rpm/5min), supernatants were collected and incubated with 2 μg of the appropriate mouse antibody and 20 μl of protein A/G agarose beads at 4 °C overnight on a roller. The agarose beads were washed five times with 1 ml of lysis buffer and then the immunoprecipitates were harvested. For Western blotting, the cell lysates and immunoprecipitates were separated by 12% SDS-PAGE, and then transferred to PVDF membranes (Millipore). Membranes were

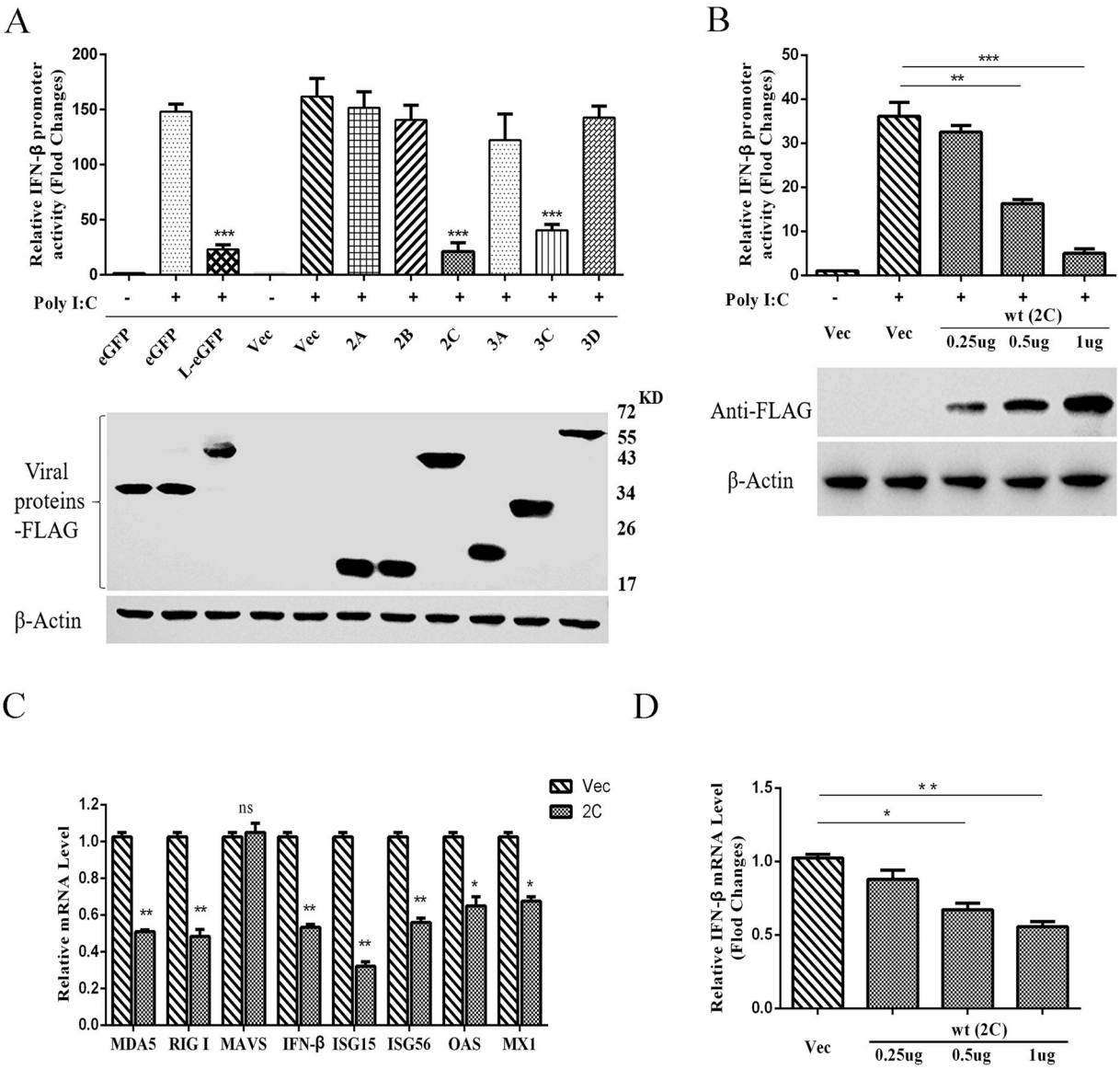

Fig. 2. Screen of the viral proteins inhibiting poly (I:C)-mediated IFN-β expression. (A) Effects of EMCV nonstructural proteins on IFN-β promoter activity induced by poly (I:C). HEK293A cells (2×10^5) were co-transfected with pIFN-β-Luc (0.4 μg), pRL-TK (10 ng as an internal control), and the indicated expression plasmids (0.6 μg) for 24 h. Cells were transfected or not transfected with poly (I:C) for 12 h, and luciferase assays were performed. (B) EMCV 2C inhibits activation of IFN-β promoter by poly (I:C) in a dose-dependent manner. Experiments similar to those in (A) were performed by using plasmid expressing 2C at different dose. (C) Effects of EMCV 2C on endogenous mRNAs levels of MDA5, RIG I, MAVS, IFN-β, ISG15, ISG56, OAS, and MX1. HEK293T cells were transfected with 1 μg EMCV 2C or empty vector (Vec) for 24 h, followed by transfection with poly (I:C) for 12 h. The mRNA levels were measured by real-time RT-PCR. (D) 2C inhibits the levels of endogenous IFN-β mRNA in a dose-dependent manner. Values are presented as mean ± SD for three independent experiments. The results are representative of three independent experiments.

blocked for 2 h in Tris-buffered saline containing 10% nonfat dry milk and 0.1% Tween-20, then incubated at 37 °C for 2 h with the appropriate primary antibody, (rabbit anti-FLAG 1:5000, rabbit anti-HA 1:5000, or rabbit anti-β-Actin 1:1000). Membranes were washed again with PBST, and incubated with HRP-labeled goat anti-rabbit antibody at 37 °C for 45 min. Membranes were treated with ECL (Thermo Fisher Scientific) and bound proteins were visualized with a Tanon 5200 chemiluminescence imaging system (Biotanon, China).

2.5. RNA isolation and qRT-PCR

Expression of mRNAs for MDA5, RIG-I, MAVS, IFN-β, ISG15, ISG56, OAS, and MX1 was detected by relative qRT-PCR. Total RNA was extracted from HEK293A cells using a Total RNA Kit I (Omega Bio-Tek) following the manufacturer's protocol. qRT-PCR was performed with SYBR Green Real-Time PCR Master Mixes (Applied Biosystems, USA) on the ABI QuantStudio 6 and 7 Real-Time PCR Systems (Applied Biosystems). β-Actin was used as the reference gene, and all data are expressed as relative fold change, as determined by the threshold cycle ($2-\Delta\Delta Ct$) method. Primer sequences for genes are shown in Table 2.

2.6. Enzyme-linked immunosorbent assay (ELISA)

PK-15, HEK-293A, and N2a cells were infected with EMCV NJ08/wt, UV-inactivated EMCV, or the EMCV 2C mutants. After infection, IFN-β levels in the cell supernatants were detected using a pig or mouse

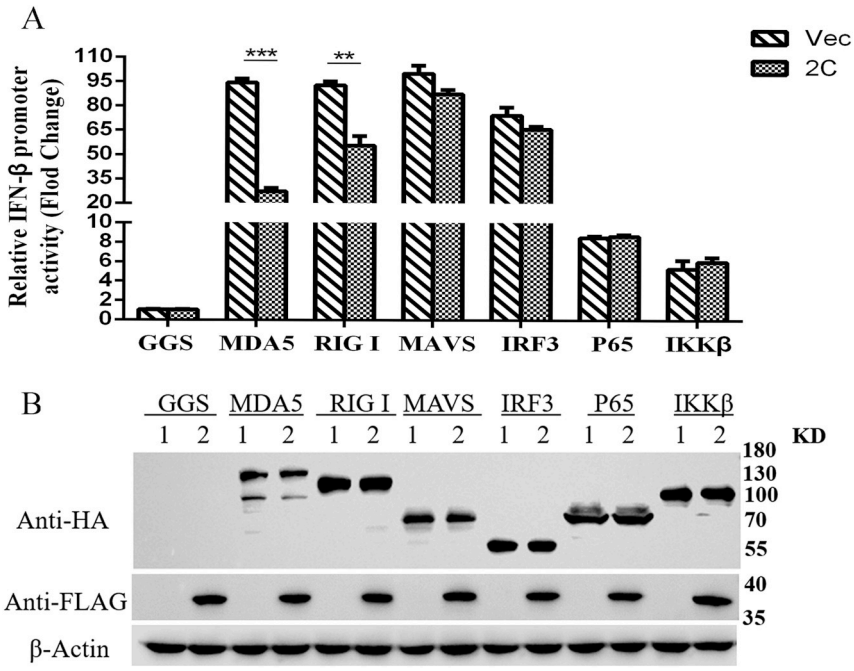

Fig. 3. EMCV $2C^{pro}$ suppresses IFN-β signaling pathway induced by MDA5 or RIG I. HEK293A cells (2×10^5) were co-transfected with IFN-β reporter (0.4 μg), 10 ng of pRL-TK (as an internal control), pCAGGS-2C (0.3 μg), and expression plasmids encoding the signaling components pCAGGS-MDA5, pCAGGS-RIG I, pCAGGS- MAVS, pCAGGS-IRF3, pCAGGS-P65, or pCAGGS-IKKβ (0.3 μg each). Luciferase assays were performed 24 h after transfection (A). Meanwhile, the levels of accumulated protein were analyzed by Western blot for all expression plasmids in transient transfection assays (B). Values are presented as the mean ± SD from three independent experiments. The results are representative of three independent experiments.

IFN-β ELISA kit, (Mlbio, Shanghai, China), or a human IFN-β ELISA kit (Elabscience, Wuhan, China), according to the instructions included with each kit.

2.7. Construction of infectious EMCV cDNA clones

The plasmid pCMV-rNJ08 (Fang et al., 2015) containing a full-length cDNA copy of EMCV strain NJ08, was used to construct EMCV 2C protein mutants. To generate the mutations, the *Nhe/SacI/Xho*I fragment containing the B fragment of EMCV was amplified from plasmid pCMV-rNJ08-B by PCR. The PCR product was cloned into pTOPO-Blunt (Aidlab Biotechnologies, China), and designated pTOPO-B2. Site-directed mutations in 2C were constructed using pTOPO-B2 and designated pTOPO-B2m. After digestion by *Nhe*I and *Sac*I, the B1 fragment was cloned into pTOPO-B2m to generate pTOPO-Bm. Finally, the *Nhe*I/*Xho*I fragment of the pCMV-rNJ08 backbone was replaced by the corresponding region from pTOPO-Bm. The full-length clone containing the mutation was designated pCMV-rNJ08/2Cm (Fig. 6A). To construct revertants, B-2Cm(R) was obtained by site-directed mutagenesis using pCMV-rNJ08/2Cm as the template.

The *Nhe*I/*Xho*I fragment of pCMV-rNJ08 was replaced with B-2Cm (R), generating pCMV-rNJ08/2Cm(R). All constructs were verified by sequencing. Plasmids of infectious cDNA clones were isolated using the QIAprep spin miniprep kit (Qiagen). All recombinant viruses and amino acid substitution primers are listed in Table 3.

To rescue viruses, BHK-21 cells were transfected with plasmids containing the full-length cDNA clones using Lipofectamine 3000 reagent and the manufacturer's protocol. When about 90% of cells exhibited cytopathic effects the supernatants were harvested then serially passaged five times in BHK-21 cells. Stocks from each passage were stored at −80 °C. The rescued viruses were designated rNJ08/wt, rV26A, rK25-3A, rV26A(R), and rK25-3A(R).

2.8. Plaque assays

Virus titers were determined by plaque assay as previously described(Fang et al., 2015). Briefly, BHK-21 cells were seeded in 12-well plates. Upon reaching confluence, the cells were inoculated with 100 $TCID_{50}$ of virus and incubated for 1 h at 37 °C. Cells were then overlaid with DMEM containing 1% low-melting-point agarose (Sigma-Aldrich) and 2% heat-inactivated FBS, and incubated 24 h. To visualize plaques, the cells were overlaid with 1% crystal violet in methanol for 4 h at 37 °C.

2.9. Viral growth curves

BHK-21 cells seeded into 24-well plates were incubated with the EMCV mutants at $10^{2.5}$ $TCID_{50}$ at 37 °C. After 1 h the inoculum was removed and fresh media was added to each well. At 5, 10, 15, 20, 25, 30, and 35 h post infection (hpi), the infected-cell supernatants were collected and stored at −70 °C for $TCID_{50}$ assay.

2.10. Statistical analysis

All data were analyzed with GraphPad Prism 5.0 using one-way ANOVA or Student's *t*-test. In graphs, error bars represent standard deviations. P-values are indicated using asterisks as *$p < 0.05$, **$p < 0.01$, and ***$p < 0.001$.

3. Results

3.1. EMCV infection antagonizes type I IFN-β expression

To determine whether EMCV affects host innate immune responses, HEK-293A cells were inoculated with live or UV-inactivated EMCV NJ08 strain. Luciferase reporter assay and ELISA results showed that EMCV infection decreased significantly IFN-β promoter activity and IFN-β expression levels in a dose-dependent manner. But UV-inactivated virus had no effect on IFN-β promoter activity and IFN-β expression (Fig. 1A and B). Meanwhile, HEK-293A cells were incubated with live or UV-inactivated EMCV and stimulated with poly (I:C). qRT-PCR results showed that the mRNA levels of MDA5, RIG-I, IFN-β, ISG15, ISG56, OAS and MX1, except MAVS, were inhibited obviously by the viral infection (Fig. 1C).

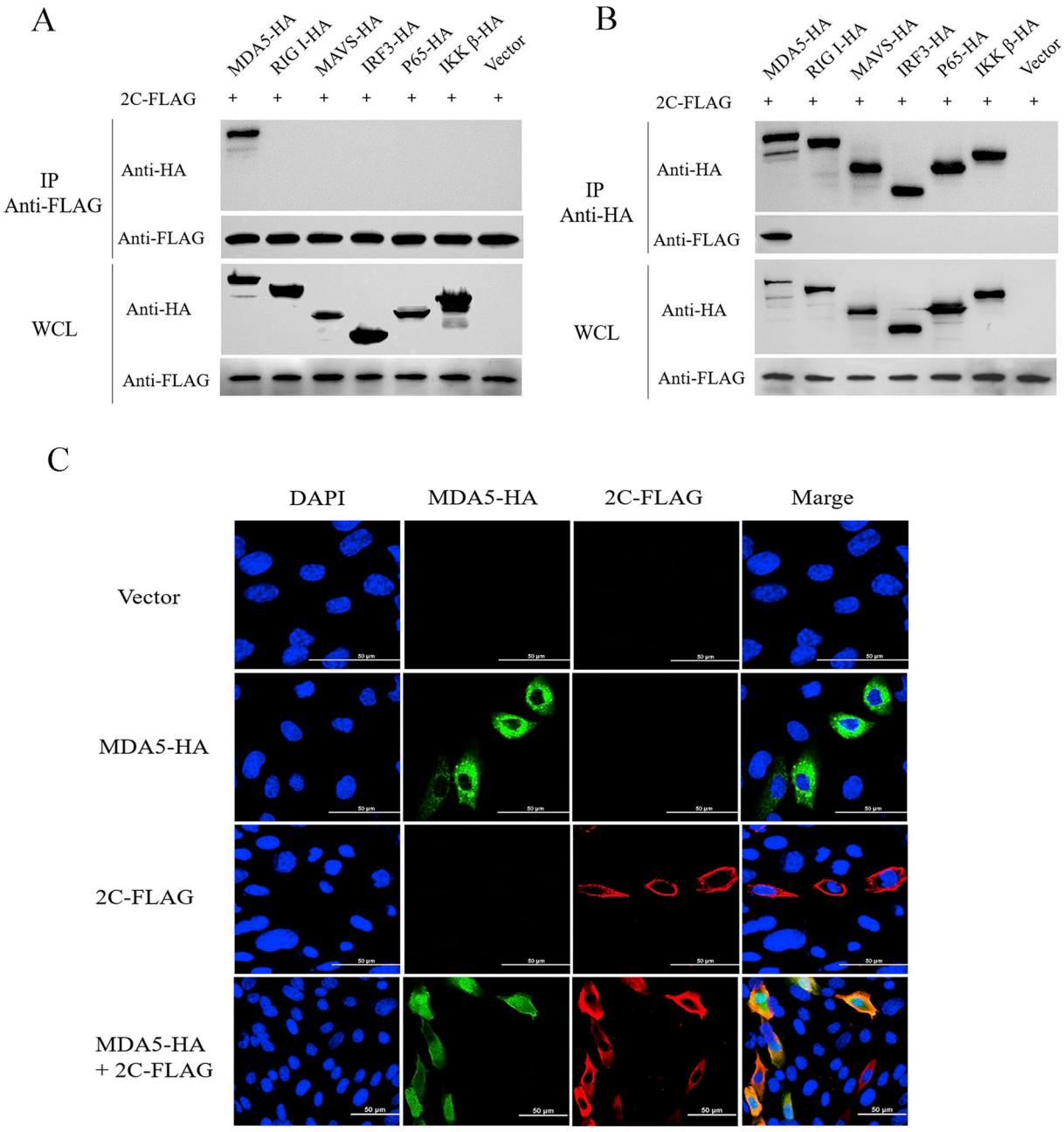

Fig. 4. EMCV 2C protein interacts with MDA5 in IFN signaling pathway. (A-B)Screen of the proteins in IFN signaling pathway interacted with EMCV 2C. HEK293A cells (1×10^6) were co-transfected with 4 μg of pCAGGS-2C-FLAG, and expression plasmids encoding the signaling components pCAGGS-MDA5, pCAGGS-RIG I, pCAGGS-MAVS, pCAGGS-IRF3, pCAGGS-P65, or pCAGGS-IKKβ (4 μg each). And the empty vector pCAGGS was used as negative control. Co-immunoprecipitations (IP) were performed with anti-FLAG mouse antibody (A) or anti-HA mouse antibody (B). Protein expression levels in the co-immunoprecipitated material were analyzed by immunoblot using the primary antibodies anti-FLAG rabbit mAbs or Anti-HA rabbit mAbs, with goat anti-rabbit antibody-HRP as the secondary antibody. WCL indicates that a whole cell lysate was analyzed rather than co-immunoprecipitated material. (C) EMCV 2C co-localizes with MDA5 in HEK293A cells. Cells were seeded onto coverslips, placed into 24-well plates, and transfected with pCAGGS-2C-FLAG and pCAGGS-MDA5-HA. After 24 h, cells were fixed for immunofluorescence assay, with 2C (red), MDA5 (green), and nuclei (blue) detected using anti-FLAG antibody, Anti-HA antibody, and DAPI, respectively. Images were obtained using confocal microscopy. The results are representative of three independent experiments.

3.2. Screen of the viral proteins inhibiting poly (I:C)-mediated IFN-β expression

To screen the nonstructural proteins of EMCV inhibiting IFN-β expression, we constructed 7 recombinant plasmids expressing viral proteins L, 2A, 2B, 2C, 3A, 3C and 3D fused with Flag (pCAGGS-L-eGFP (expressing L protein fused with eGFP), pCAGGS-2A, pCAGGS-2B, pCAGGS-2C, pCAGGS-3A, pCAGGS-3C and pCAGGS-3D) and confirmed with Western blotting (Fig. 2A). HEK-293A cells were co-transfected with the plasmids, together with pIFN-β-luc (containing IFN-β promoter) and pRL-TK, and treated with poly (I:C). Luciferase assays results show that L-eGFP, 2C and 3C proteins markedly inhibit poly (I:C)-

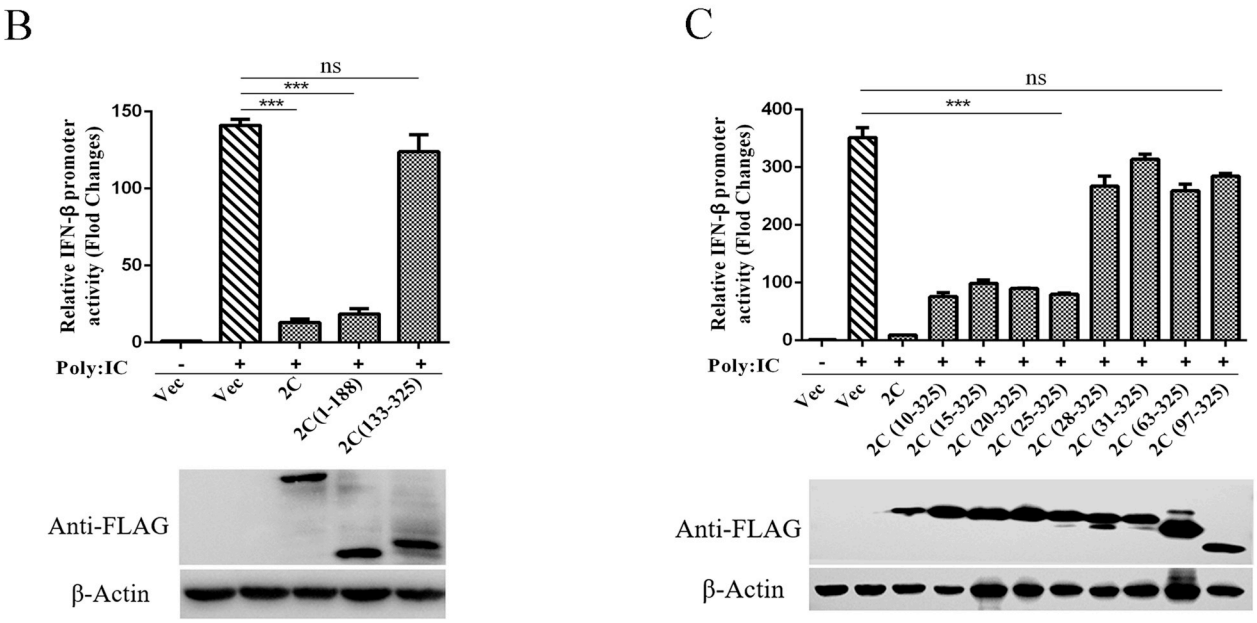

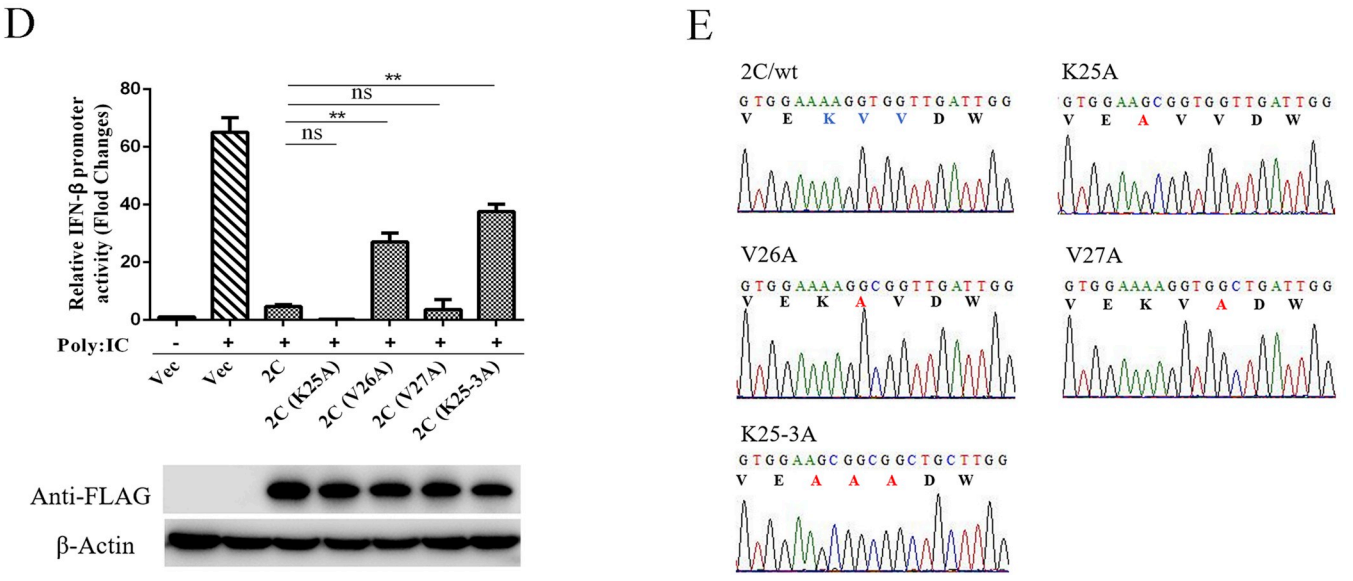

(caption on next page)

Fig. 5. Mutations in 2C decrease the inhibition of IFN-β promoter activity. (A) Construct of EMCV 2C mutants that showing regions retained relative to the wild type (wt) 2C protein. (B–D) Effects of the mutations in 2C on IFN-β promoter activity induced by poly (I:C). HEK293A (2×10^5) cells were transfected with pIFN-β-luc (0.4 μg), pRL-TK (0.1 μg) together with wt 2C or mutant 2C expression plasmids (0.6 μg), which including truncated 2C (B), mutants with single alanine substitutions at positions 25 to 27aa (C), and a mutant with multiple alanine substitutions at positions 25 through 27 aa (D). 24 h after transfection, cells were transfected with poly (I:C) or were left untransfected for 12 h before luciferase assays were performed. Cells transfected with pCAGGS served as a negative control, and cells transfected with pCAGGS and then transfected with poly (I:C) 12 h prior to harvest served as a positive control. Protein expression in cell lysates was measured by Western blot using Anti-FlAG antibody. β-Actin was used as a loading control. (E) Sequencing chromatogram of 2C wild-type and its mutants. Values are presented as the mean ± SD from three independent experiments.

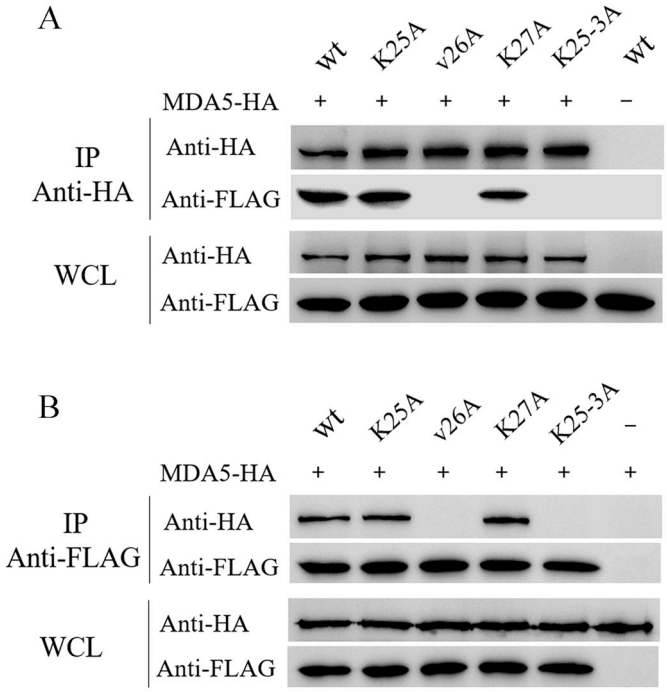

Fig. 6. Mutants V26A and K25-3A lost the ability to interact with MDA5. HEK293A cells (1×10^6) were transfected with recombinant plasmid pCAGGS-MDA5-HA, together with the plasmids expressing 2Cwt, K25A, V26A, V27A or K25-3A fused with Flag at dose of 4 μg. And the empty vector pCAGGS was used as negative control. After incubated for 24 h, the cells were collected and co-immunoprecipitations (IP) were performed with anti-HA mouse antibody (A). In another experiment, the cells were collected and co-immunoprecipitations (IP) were performed with anti-FlAG mouse antibody (B). Protein expression levels in the co-immunoprecipitated material were analyzed by immunoblot using the primary antibodies anti-HA rabbit mAbs or Anti-FLAG rabbit mAbs, with goat anti-rabbit antibody-HRP as the secondary antibody. WCL indicates that a whole cell lysate was analyzed rather than co-immunoprecipitated material. The results are representative of three independent experiments.

mediated IFN-β promoter activity (Fig. 2A).

Furthermore, Luciferase assays results show that the viral 2C reduces IFN-β promoter activity in a dose-dependent manner (Fig. 2B). After transfection with pCAGGS-2C and treated with poly (I:C) in HEK293 cells,qRT-PCR results show that the levels of MDA5, RIG-I, IFN-β, ISG15, ISG56, OAS, and MX1, except MAVS, were inhibited significantly by the viral 2C protein (Fig. 2C). And the viral 2C decreases IFN-β mRNA levels in a dose-dependent manner (Fig. 2D). These results show that $2C^{pro}$of EMCV antagonizes poly (I:C)-induced IFN-β induction.

3.3. EMCV $2C^{pro}$ suppresses IFN-β signaling pathway induced by MDA5 or RIG-I

To explore the signaling pathway affected by viral protein 2C, six recombinant plasmids(pCAGGS-MDA5, pCAGGS-RIG-I, pCAGGS-MAVS, pCAGGS-IRF3, pCAGGS-P65, and pCAGGS-IKKβ, expressing MDA5, RIG-I, MAVS, IRF3, P65, and IKKβ in the IFN-β signaling pathway) were constructed and confirmed by Western blotting (Fig. 3B). After co-transfection with the plasmids, and pCAGGS-2C, pIFN-β-luc and pRL-TK, Luciferase assays results indicate that EMCV 2C inhibits the IFN-β promoter in the presence of MDA5 and RIG-I, but not in MAVS or its downstream components IRF3, P65, or IKKβ (Fig. 3A). These results suggest that the 2C protein of EMCV affects inhibition of the type I IFN signaling pathway by MDA5 or RIG-I.

3.4. Screen of the proteins in IFN signaling pathway interacted with EMCV $2C^{pro}$

In order to screen the proteins interacted with EMCV 2C protein, HEK-293A cells were co-transfected with pCAGGS-2C and the recombinant plasmids expressing MDA5, RIG-I, MAVS, IRF3, P65 or IKKβ. Co-immunoprecipitation experiment results showed that EMCV 2C interacts with MDA5 specifically, but not with RIG-I, MAVS, IRF3, P65 or IKKβ (Fig. 4A and B). Furthermore, confocal microscopy results showed that EMCV 2C and MDA5 are co-located in the cytoplasm of HEK-293A cells (Fig. 4C). These results suggest that EMCV 2C targets and interacts with MDA5 in HEK-293A cells.

3.5. Mutations in 2C decrease the inhibition of IFN-β promoter activity

To identify the key amino acid (aa) residues in 2C that are involved in suppressing IFN-β production, two truncation mutants were constructed from the full-length 2C gene using PCR and designated 2C(1-188aa) and 2C(133-325aa) (Fig. 5A). Luciferase assays showed that only the N-terminal 188 aa of EMCV 2C suppress poly (I:C)-induced IFN-β promoter activation (Fig. 5B).

To examine the N-terminal region at higher resolution, eight N-terminal truncates were generated and identified. Luciferase assays results showed that 2C(10-325aa), 2C(15-325aa), 2C(20-325aa), and 2C(25-325aa) mutants inhibit IFN-β promoter activity, but 2C(28-325aa), 2C(31-325aa), 2C(63-325aa), and 2C(97-325aa) do not (Fig. 5A and C).

Subsequently, single and multi-nucleotide alanine substitution mutants were constructed, generating plasmids K25A, V26A, V27A, and K25-3A. Sequencing chromatogram of the wt and mutants are shown in Fig. 5E. Luciferase assays results showed that V26A and K25-3A mutants decrease significantly the inhibition of IFN-β promoter activity compared with wt $2C^{pro}$ And K25A and V27A mutants, although they still had the inhibition ability of IFN-β promoter activity (Fig. 5D). The results indicate that amino acids 26 in the N-terminus of EMCV 2C play an important role in inhibiting type I IFN promoter activity.

3.6. Mutants V26A and K25-3A lost the ability to interact with MDA5

HEK-293A cells were co-transfected with pCAGGS-***MDA5*** and the recombinant plasmids expressing K25A, V26A, V27A, K25-3A or wt 2C. Co-immunoprecipitation experiment results showed wt, K25A and V27A specifically interact with MDA5, but V26A and K25-3A do not interact with MDA5 (Fig. 6A and B). These results show that amino acids 26 of 2C play a crucial role in antagonizing IFN-β induction.

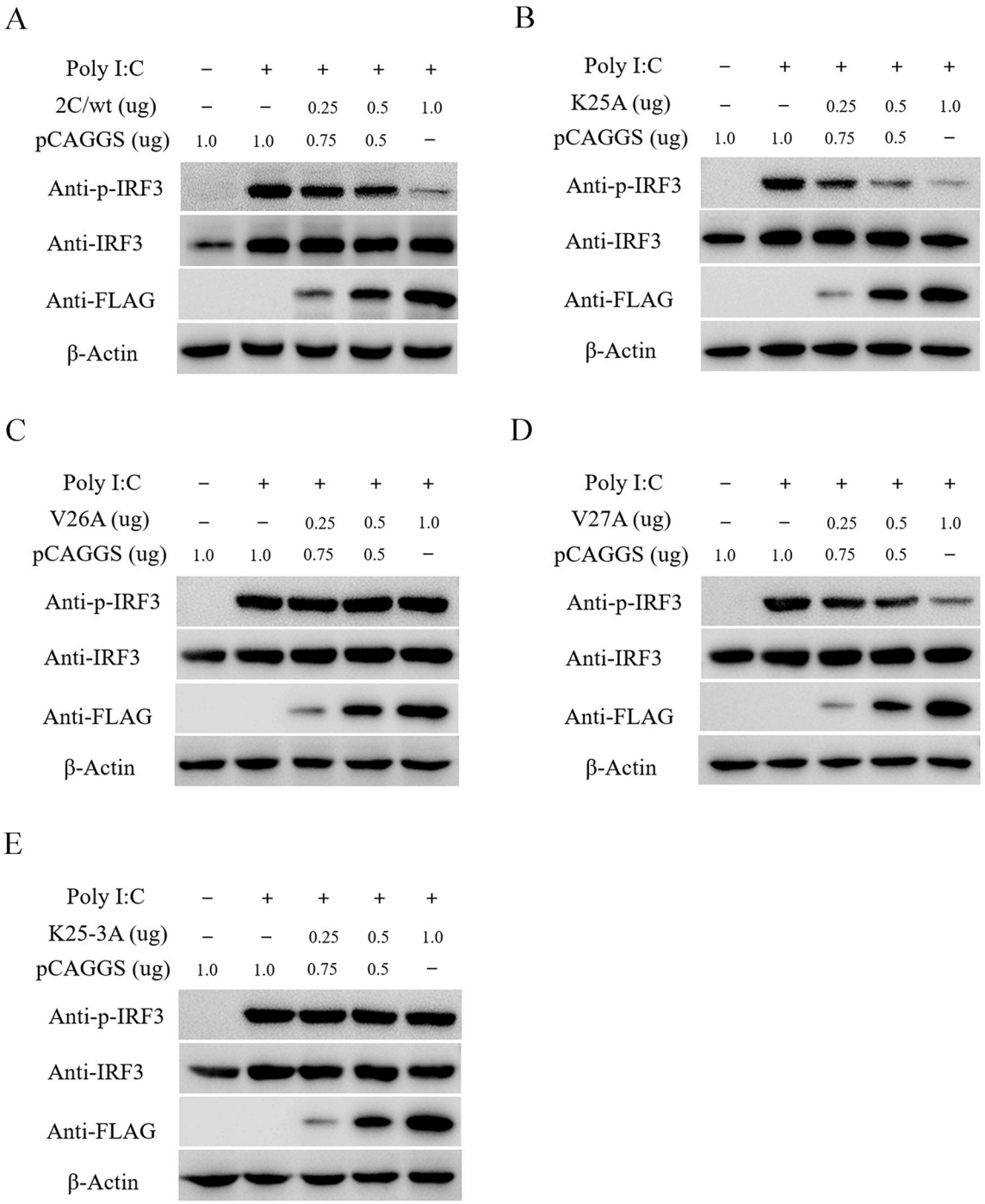

Fig. 7. Effect of 2C and its mutations on poly (I:C)-mediated IRF3 phosphorylation. HEK293A (1×10^6) cells were co-transfected with an increasing amount of the plasmids expressing wt 2C, K25A, V26A, V27A or K25-3A fused with Flag and corresponding amount of empty vector pCAGGS. After incubated for 24 h, cells were transfected with poly (I:C) or were left untransfected. And 12 h later, the cells were collected and IRF3 phosphorylation was detected by using Western blotting with anti-p-IRF3 antibody. Meanwhile, IRF3, 2C and β-Actin proteins were also detected by Western blotting. The results are representative of three independent experiments.

3.7. Effect of 2C and its mutations on poly (I:C)-mediated IRF3 phosphorylation

After transfection with wt 2C, K25A, V26A, V27A, and K25-3A plasmids in HEK-293A cells, individually, and stimulated with poly (I:C), the cells were collected for Western blotting. The results showed that phosphorylation levels of IRF3 significantly decreased in wt 2C in a dose-dependent manner (Fig. 7A). But the phosphorylation levels of IRF3 do not changed obviously in V26A and K25-3A, compared with those in wt 2C, K25A and V27A expressed cells (Fig. 7B and C D). It suggests that EMCV 2C mutants (V26A and K25-3A) abolished the effect of reducing the phosphorylation of IRF3 (Fig. 8).

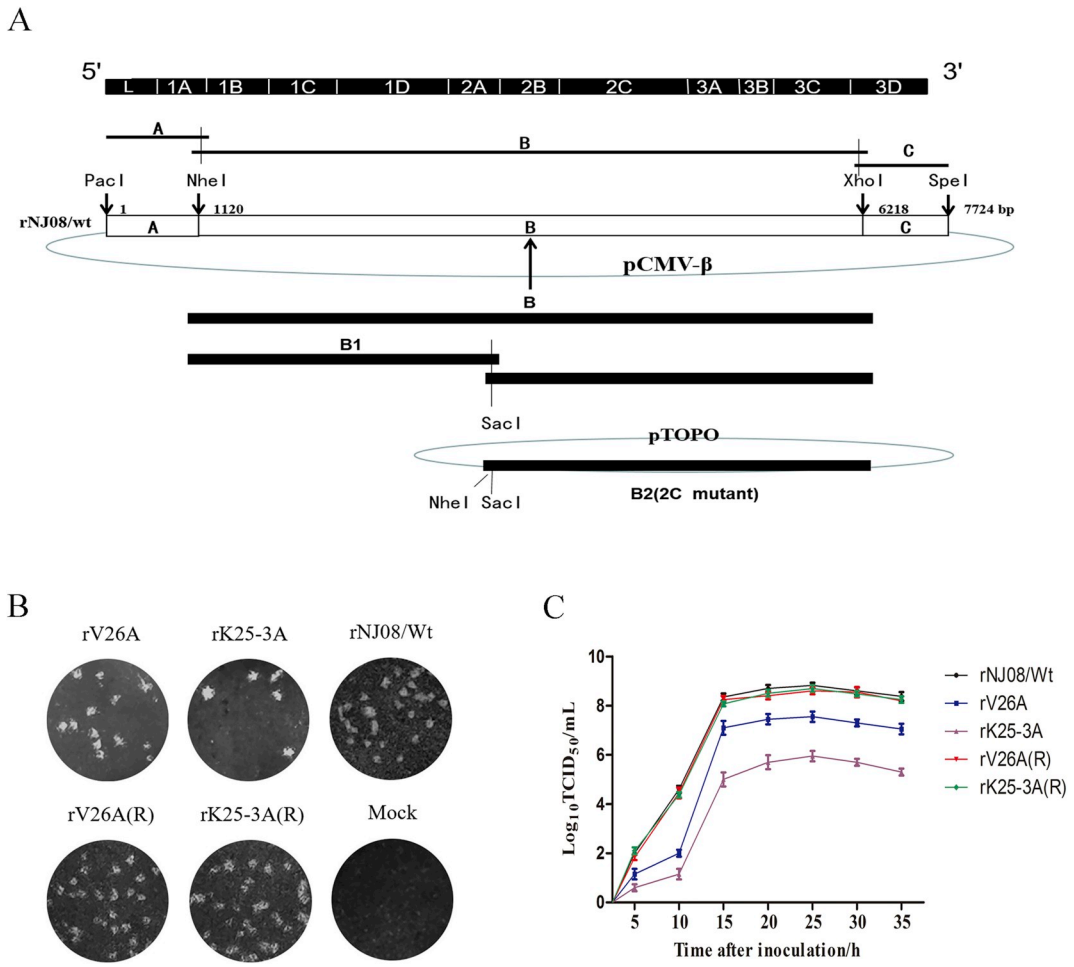

Fig. 8. Construction and identification of recombinant EMCV with mutations in 2C protein. (A) Construction of full-length cDNA clones and two rescued EMCV strains containing mutations in 2C. (B) Plaque morphology of rescued viruses in BHK-21 cells. Cells in 12-well plates were infected with the wild-type rNJ08/wt strain or with mutant virus, cultured in DMEM with a 1% agarose overlay, fixed 24 h after infection, and stained with 1% crystal violet. (C) One-step growth curves for rescued viruses. BHK-21 cells were infected with parental rNJ08 or mutants at a load of 100 $TCID_{50}$. Culture supernatants were collected at the indicated time points (hpi), and virus titers determined using $TCID_{50}$ assay. Values are presented as the mean ± SD from three independent experiments.

3.8. Construction and identification of recombinant EMCV 2C^{pro} mutants and their revertants

To confirm the foundation of residues 25-27aa of 2C, the recombinant EMCV with 2C mutations at residues 25-27aa were constructed by using EMCV infectious cDNA clones. Mutations rV26A and rK25-3A, which cause cytopathic effects in BHK-21 cells, were recovered. And their revertants, rV26A(R) and rK25-3A(R), were rescued from the corresponding rV26A and rK25-3A infectious cDNA clones. As shown in Fig. 6B, plaque formation by rV26A, rK25-3A, rV26A(R), and rK25-3A(R) was similar to that by wild type virus in BHK-21 cells. However, the titres of plaques formed by rV26A and rK25-3A were less than those formed by rV26A(R), rK25-3A(R), and wild-type rNJ08/wt. In addition, rV26A and rK25-3A grew more slowly than rNJ08/wt and the revertants rV26A(R) and rK25-3A(R).

3.9. Effects of EMCV mutants on IFN-β promoter activity and phospho-IRF3 in HEK-293A cells

HEK-293A cells were co-transfected with plasmids pGL3-IFN-β-Luc and pRL-TK, and infected with rNJ08/wt and its mutant viruses rV26A, rK25-3A, rV26A(R) or rK25-3A(R) and treated with poly (I:C). Luciferase assays revealed that rNJ08/wt or rV26A(R) and rK25-3A(R) suppressed obviously IFN-β promoter activity, but rV26A and rK25-3A do not (Fig. 9A).

The phosphorylation levels of IRF3 during those viral infections in HEK-293A cells were also detected as above. As shown in Fig. 9B, IRF3 was phosphorylated in mock-infected cells mediate by poly (I:C). rNJ08/wt, rV26A(R) and rK25-3A(R) infection obviously decrease phospho-IRF3. But the phosphorylation levels of IRF3 were not decreased in rV26A and rK25-3A. It suggests that EMCV mutants rV26A and rK25-3A up-regulate type I IFN signaling.

3.10. Effects of EMCV mutants on IFN-β signaling pathway in different cells lines

PK-15, HEK-293A and N2a cells were used to be infected with EMCV mutants and then IFN-β expression levels were measured by qRT-PCR and ELISA. As shown in Fig. 10A and B, the levels of IFN-β production in rV26A and rK25-3A were significantly higher than those in rNJ08/wt, rV26A(R), and rK25-3A(R) in PK-15 cells ($P < 0.01$). Similar results were observed in HEK-293A cells and in N2a cells.

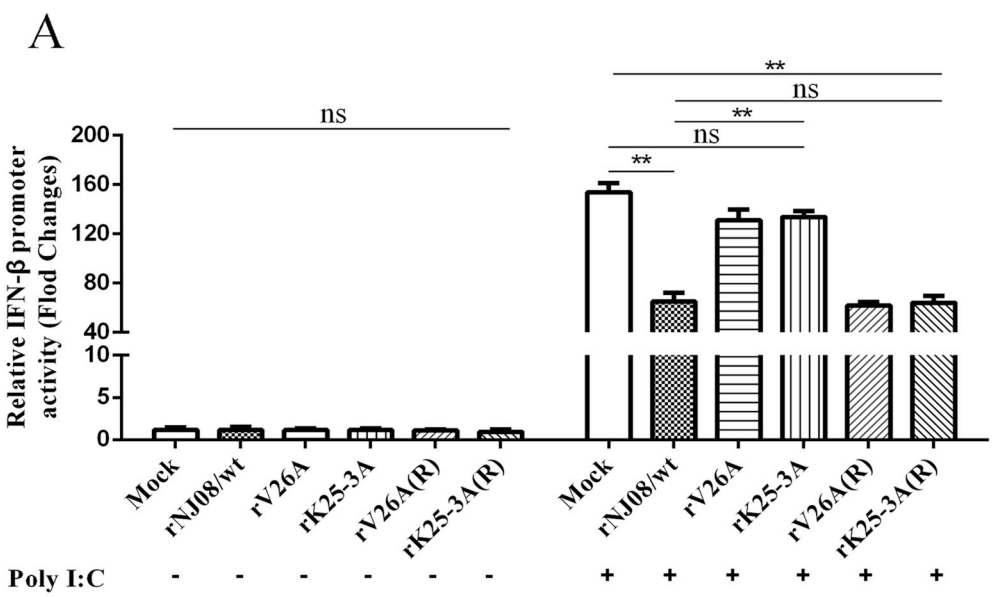

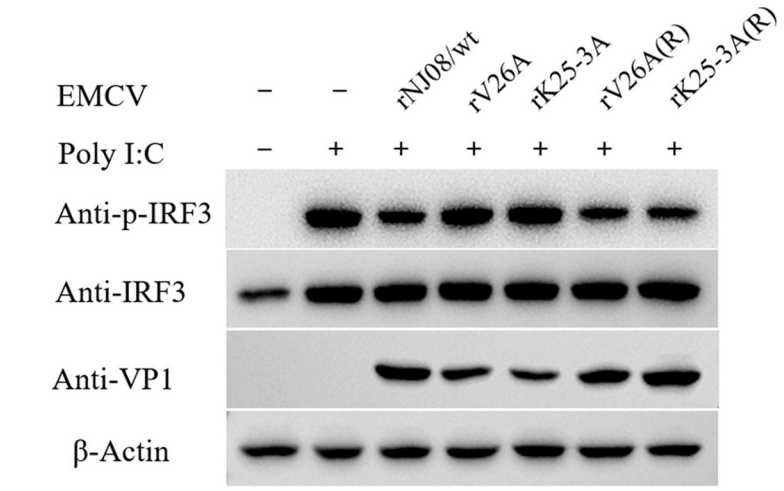

Fig. 9. Effects of EMCV mutants on IFN-β promoter activity and phospho-IRF3 in HEK-293A cells. (A) HEK-293A cells (2×10^5) were transfected with 400 ng of pIFN-β-luc plasmid and 10 ng of pRL-TK plasmid. At 24 hpt, the cells were mock-infected or infected with EMCV NJ08/wt or its mutants at an MOI of 0.1, respectively. At 3 hpi, the cells were stimulated or unstimulated with poly (I:C) for 12 h and luciferase assays were performed. (B) HEK-293A cells (1×10^6) were mock-infected or infected with EMCV NJ08/wt or its mutants at an MOI of 0.1. Then transfected or were untransfected with poly (I:C). At 12 hpt, the cells were collected and IRF3 phosphorylation was detected by using Western blotting with anti-p-IRF3 antibody. Meanwhile, IRF3, viral VP1 and β-Actin proteins were also detected by Western blotting. The results are representative of three independent experiments.

Meanwhile, those virus infections were analyzed by Western blotting with an anti-VP1 protein monoclonal antibody (Fig. 10C).

In parallel experiments, the mRNA expression levels of ISG15, ISG56, OAS, and MX1 were detected by qRT-PCR in PK-15, HEK-293A and N2a cells. The results showed that the mRNA levels of ISG15, ISG56, and OAS induced by rV26A and rK25-3A were significantly higher than those induced by rV26A(R), rK25-3A(R), and rNJ08/wt ($p < 0.01$) (Fig. 11A–D). And all the virus infections in different cells were confirmed by Western blotting (Fig. 11E). These results indicate that residues V26 and K25-27 of EMCV 2C play an important role in inhibiting type I IFN expression (see Fig. 12).

4. Discussion

The innate immune response system is the first line of defense that is activated after infection by a virus. At this stage, the IFN signaling pathway plays a crucial role in enabling the expression of a set of antiviral genes that are responsible for antiviral effects. However, many viruses can escape the innate immune response because they have evolved antagonistic mechanisms. For example, FMDV 3A protein inhibits MDA5, RIG-I, and MAVS mRNAs by interacting with them, thereby suppressing the IFN-β signaling pathway (Li et al., 2016a). FMDV 2B protein can decrease RIG-I expression and evade the RIG-I-mediated innate immunity response (Zhu et al., 2016).

EMCV, a member of the *Picornaviridae* family, also has the ability to escape the type I IFN signaling pathway. EMCV 3C can cleave TANK, a TRAF-binding protein, and activate NF-κB signaling in TRAF2-transfected cells (Li et al., 2017; Yang et al., 2008). This disables the TANK–TBK1–IKKε–IRF3 complex, attenuates IRF3 phosphorylation, and ultimately reduces type I IFN production (Huang et al., 2017). In this study, we showed that IFN-β transcription level and IFN-β production are suppressed during EMCV infection in HEK-293A cells. This immunosuppression may occur because the host initially recognizes the invasion of the virus and the innate immune response is suppressed after the virus invades.

We found that the 2C protein of EMCV plays an important role in inhibiting the activation of the type I IFN signaling pathway by interacting with the MDA5 protein. RIG-I and MDA5 are the crucial factors

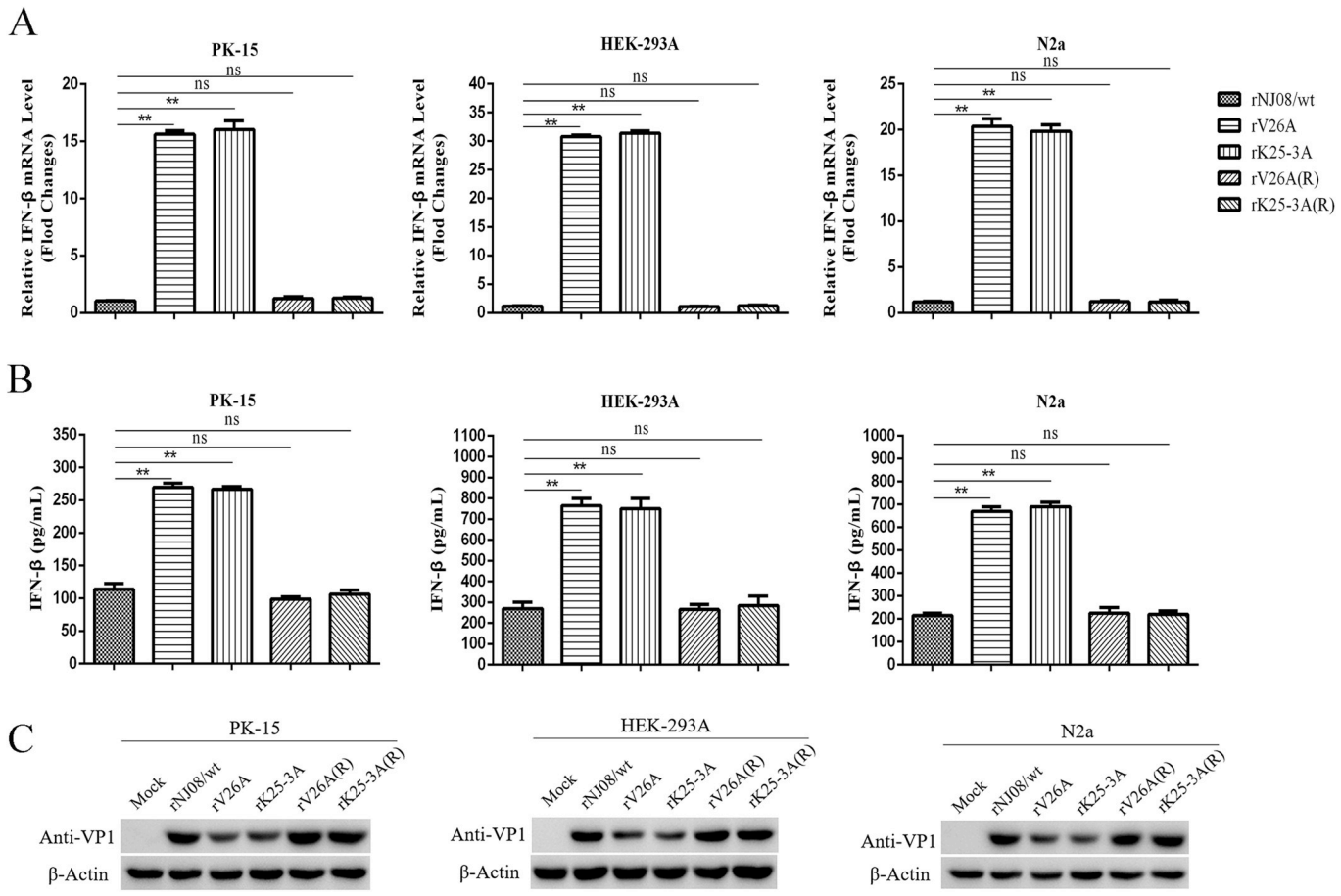

Fig. 10. Effects of EMCV mutants on the IFN-β production in PK-15, HEK-293A, and N2a cells. PK-15, HEK-293A, and N2a cells were infected with recombinant EMCV [rNJ08/wt, rV26A, rK25-3A, rV26A(R), or rK25-3A(R)] at an MOI of 0.1. After incubation for 3 h, the cells were stimulated with poly (I:C) for 12 h, IFN-β production and mRNA levels were measured by ELISA (A) and qRT-PCR (B). Meanwhile, the viral protein VP1 and β-actin were detected by using Western blotting with anti-VP1 and β-actin antibodies (C). Values are presented as the mean ± SD from three independent experiments.

that identify virus nucleic acid in infected cells. However, in a picornavirus infection, viral RNA is primarily detected by MDA5 rather than RIG-I (Feng et al., 2012a; Triantafilou et al., 2012a). MDA5 plays an essential role in antagonizing the picornavirus. The blocking of MDA5 function may occur through multiple mechanisms. Enterovirus 71 (EV71) and Coxsackievirus B3 (CVB3) infection can induce MDA5 expression via the viral 2A protein. In coxsackieviruses and enteroviruses such as CV-A16, CV-A6, and EV-D68, the 3C protein disrupts the function of MDA5 by directly interfering with MDA5-MAVS signal transduction. Some paramyxoviruses, including SeV, human parainfluenza virus 2, hendra virus and mumps virus, disrupt MDA5-mediated antiviral functions as a result of interaction between the viral V protein and MDA5. In this study, we analyzed 7 recombinant plasmids that express the L-eGFP, 2A, 2B, 2C, 3A, 3C, and 3D proteins of EMCV, and found that L-eGFP^{pro}, 2C^{pro} and 3C^{pro} strongly inhibit the activation of IFN-β promoter by poly (I:C) (Fig. 2A). Here, we focused on 2C protein of EMCV. Our results show that 2C protein can interact with MDA5 to suppress MDA5-mediated IFN-β promoter activity. We also detected IFN-β promoter induction by MAVS, IRF3, P65, and IKKβ, but the promoter activation in these cases is not affected by 2C. The results suggest that EMCV 2C specifically inhibits the MDA5-mediated IFN-β signaling pathway by interacting with MDA5 and disrupting its normal function. Moreover, we detected 2C also inhibits RIG-I-mediated promoter activity, but cannot interact with RIG-I. Therefore, the mechanism of 2C protein inhibiting RIG-I- mediated IFN-β promoter activity needs further exploration.

Many viruses encode proteins that function antagonistically against innate immune responses. The mechanisms underlying viral antagonism can be explored by examining sub-regions within each protein using genetic manipulation. For example, the region comprising amino acids 1–51 of FMDV 3A is essential for inhibiting the IFN-β signaling pathway, because it interacts with MDA5, RIG-I, and MAVS. FMCV 2B amino acids 105-114 and 135-144 interact with RIG-I, resulting in the degradation of RIG-I (Zhu et al., 2016). To identify the regions by which 2C protein inhibits activation of the type I IFN promoter, we constructed ten domain-specific mutants, and found that the region spanning amino acids 25-27 plays an important role (Fig. 5C). Amino acid 26 (V26) was confirmed as the key residue that inhibits activation of the IFN production by poly (I:C). Using cDNA infectious clones, two recombinant viruses with mutations at residues 26 and 25-27 (rV26A and rK25-3A), and their revertants rV26A(R) and rK25-3A(R), were rescued. Mutants rV26A and rK25-3A were partially impaired in their ability to inhibit type I IFN production, indicating that V26 is necessary for suppression of the IFN-β signaling pathway. rV26A as well as rK25-3A exhibited slow growth kinetics in BHK-21 cells, and rK25-3A reached a maximum titer of only $10^{5.5}$ $TCID_{50}$/ml. This suggests that V26 in 2C is also necessary for EMCV replication.

In summary, we firstly found that EMCV 2C protein is a novel type I IFN antagonist, and suppresses activation of the innate immune response by interacting with MDA5. The amino acid V26 in 2C plays a crucial role in inhibiting the IFN-β signaling pathway. These results reveal a new molecular mechanism by which EMCV evades host innate immunity.

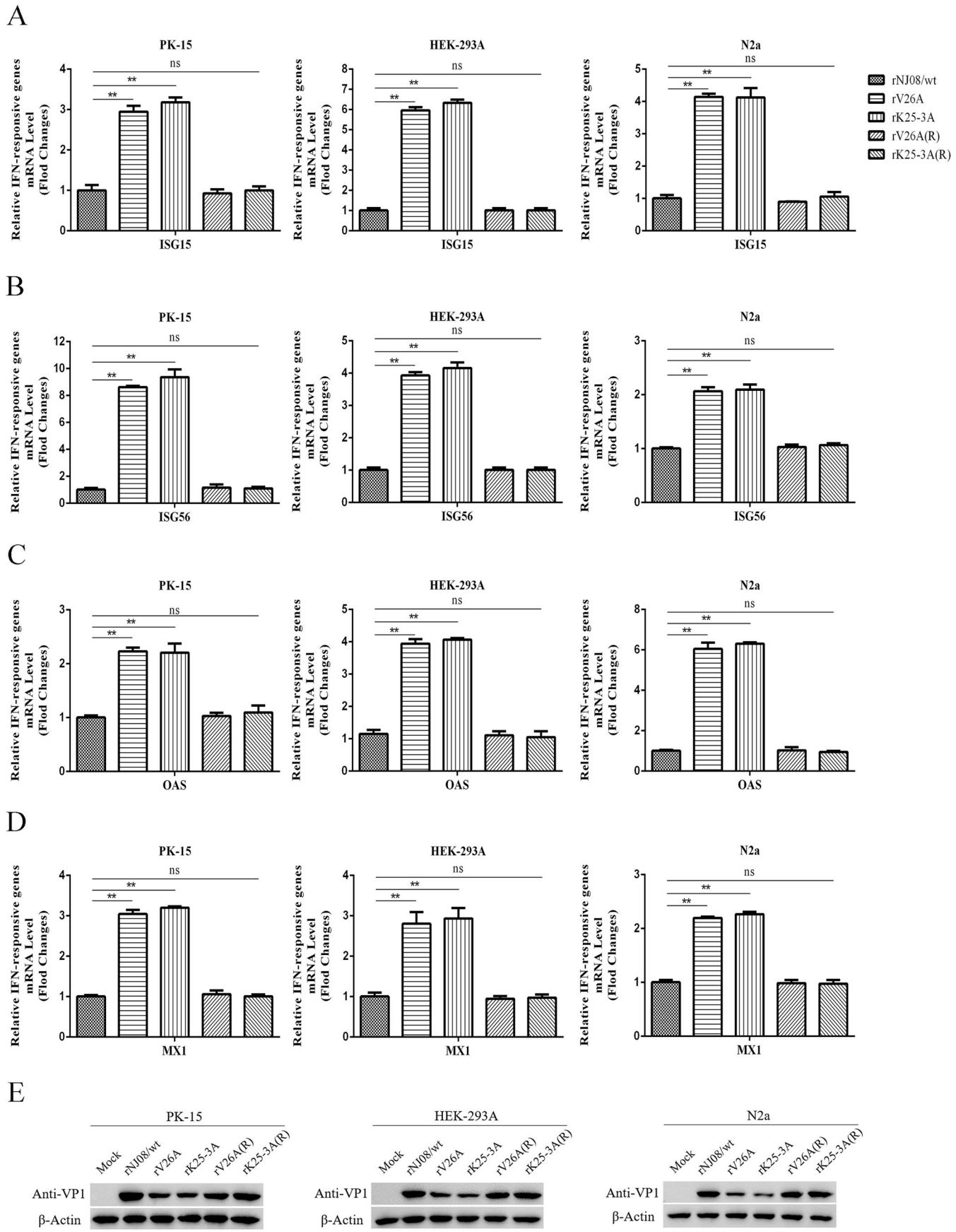

Fig. 11. Effects of EMCV mutants on IFN-β signaling pathway in PK-15, HEK-293A, and N2a cells. PK-15, HEK-293A, and N2a cells were infected with recombinant EMCV [rNJ08/wt, rV26A, rK25-3A, rV26A(R), or rK25-3A(R)] at an MOI of 0.1. After incubation for 3 h, the cells were transfected with poly (I:C) for 12 h, the mRNA levels of ISG15 (A), ISG56 (B), OAS (C) and Mx1 (D) in IFN-β signaling pathway, were quantified by real-time PCR. Meanwhile, the viral protein VP1 and β-actin were detected by using Western blotting with anti-VP1 and β-actin antibodies (E). Values are presented as the mean ± SD from three independent experiments.

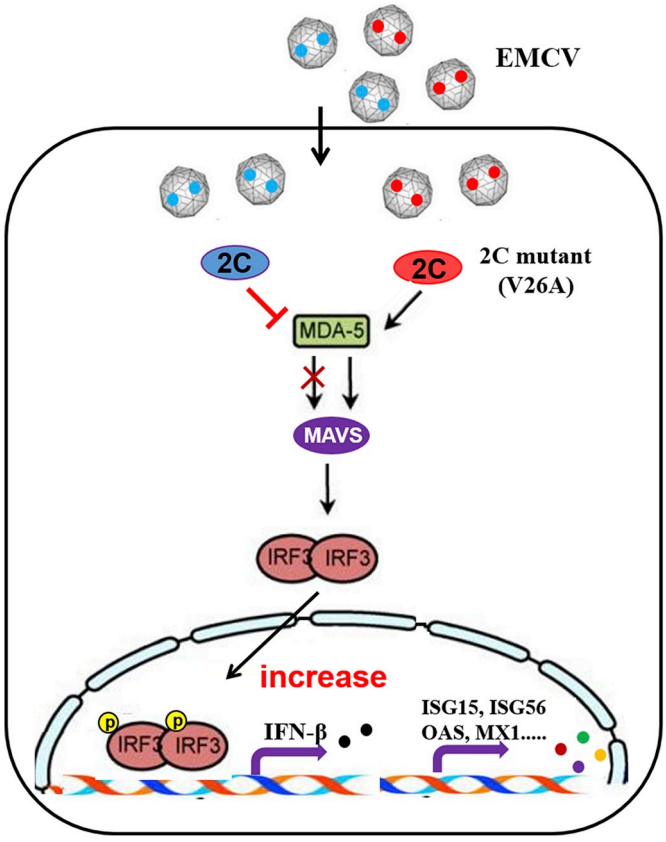

Fig. 12. The model of EMCV-mediated inhibition of type I IFN signaling. After EMCV infection, the intracellular accumulation of viral protein 2C interacts and inhibits MDA5 activation, suppresses the phosphorylation of IRF3 and ultimately blocks the IFN-β production. Furthermore, the transcriptional levels of ISG15, ISG56, OAS and MX1 were decreased. However, mutations in V26A and K25-3A of 2C (rV26A and rK25-3A) lost its ability to inhibition of the type I IFN signaling.

Conflicts of interest

None of the authors have any possible conflicts of interest.

Acknowledgments

This work was supported by the National Natural Science Foundation (31502082) and this Foundation supported by the Fundamental Research Funds for the Central Universities (KJQN201616), a Jiangsu Natural Science Foundation Award for Young Researchers (BK20130691), an award from the Ministry of Agriculture (CARS-36) to develop techniques for the control of swine disease, and an award from the Priority Academic Program Development of Jiangsu Higher Education Institutions (PAPD).

References

Akira, S., Uematsu, S., Takeuchi, O., 2006. Pathogen recognition and innate immunity. Cell 124 (4), 783–801.
Banerjee, R., Tsai, W., Kim, W., Dasgupta, A., 2001. Interaction of poliovirus-encoded 2C/2BC polypeptides with the 3' terminus negative-strand cloverleaf requires an intact stem-loop b. Virology 280 (1), 41–51.
Carocci, M., Bakkali-Kassimi, L., 2012. The encephalomyocarditis virus. Virulence 3 (4), 351–367.
Darnell, J.J., 1998. Studies of IFN-induced transcriptional activation uncover the Jak-Stat pathway. J. Interferon Cytokine Res. 18 (8), 549–554.
Fang, P., Bai, J., Liu, X., Dong, J., Sun, T., Jiang, P., 2015. Construction and characterization of an infectious cDNA clone of encephalomyocarditis virus from pigs in China. Arch. Virol. 160 (3), 805–809.
Feng, Q., Hato, S.V., Langereis, M.A., Zoll, J., Virgen-Slane, R., Peisley, A., Hur, S., Semler, B.L., van Rij, R.P., van Kuppeveld, F.J., 2012a. MDA5 detects the double-stranded RNA replicative form in picornavirus-infected cells. Cell Rep. 2 (5), 1187–1196.
Fitzgerald, M.E., Rawling, D.C., Vela, A., Pyle, A.M., 2014. An evolving arsenal: viral RNA detection by RIG-I-like receptors. Curr. Opin. Microbiol. 20, 76–81.
Garcia-Sastre, A., Biron, C.A., 2006a. Type 1 interferons and the virus-host relationship: a lesson in detente. Science 312 (5775), 879–882.
Glatt, S., Baeten, D., Baker, T., Griffiths, M., Ionescu, L., Lawson, A., Maroof, A., Oliver, R., Popa, S., Strimenopoulou, F., Vajjah, P., Watling, M., Yeremenko, N., Miossec, P., Shaw, S., 2017. Dual IL-17A and IL-17F neutralisation by bimekizumab in psoriatic arthritis: evidence from preclinical experiments and a randomised placebo-controlled clinical trial that IL-17F contributes to human chronic tissue inflammation. Ann. Rheum. Dis. 77 (4), 523–532.
Hindiyeh, M., Li, Q.H., Basavappa, R., Hogle, J.M., Chow, M., 1999. Poliovirus mutants at histidine 195 of VP2 do not cleave VP0 into VP2 and VP4. J. Virol. 73 (11), 9072–9079.
Hou, L., Ge, X., Xin, L., Zhou, L., Guo, X., Yang, H., 2014. Nonstructural proteins 2C and 3D are involved in autophagy as induced by the encephalomyocarditis virus. Virol. J. 11, 156.
Huang, L., Xiong, T., Yu, H., Zhang, Q., Zhang, K., Li, C., Hu, L., Zhang, Y., Zhang, L., Liu, Q., Wang, S., He, X., Bu, Z., Cai, X., Cui, S., Li, J., Weng, C., 2017. Encephalomyocarditis virus 3C protease attenuates type I interferon production through disrupting the TANK-TBK1-IKKepsilon-IRF3 complex. Biochem. J. 474 (12), 2051–2065.
Ito, M., Yanagi, Y., Ichinohe, T., 2012. Encephalomyocarditis virus viroporin 2B activates NLRP3 inflammasome. PLoS Pathog. 8 (8), e1002857.
Kang, D.C., Gopalkrishnan, R.V., Wu, Q., Jankowsky, E., Pyle, A.M., Fisher, P.B., 2002. mda-5: an interferon-inducible putative RNA helicase with double-stranded RNA-dependent ATPase activity and melanoma growth-suppressive properties. Proc. Natl. Acad. Sci. U. S. A. 99 (2), 637–642.
Li, D., Lei, C., Xu, Z., Yang, F., Liu, H., Zhu, Z., Li, S., Liu, X., Shu, H., Zheng, H., 2016a. Foot-and-mouth disease virus non-structural protein 3A inhibits the interferon-beta signaling pathway. Sci. Rep. 6, 21888.
Li, S., Lu, L.F., LaPatra, S.E., Chen, D.D., Zhang, Y.A., 2017. Zebrafish STAT6 negatively regulates IFNphi1 production by attenuating the kinase activity of TANK-binding kinase 1. Dev. Comp. Immunol. 67, 189–201.
Loughran, G., Firth, A.E., Atkins, J.F., 2011. Ribosomal frame shifting into an overlapping gene in the 2B-encoding region of the cardiovirus genome. Proc. Natl. Acad. Sci. U. S. A. 108 (46), E1111–E1119.
Medzhitov, R., Janeway, C.J., 2002. Decoding the patterns of self and nonself by the innate immune system. Science 296 (5566), 298–300.
Sato, M., Tanaka, N., Hata, N., Oda, E., Taniguchi, T., 1998. Involvement of the IRF family transcription factor IRF-3 in virus-induced activation of the IFN-beta gene. FEBS Lett. 425 (1), 112–116.
Stetson, D.B., Medzhitov, R., 2006. Type I interferons in host defense. Immunity 25 (3), 373–381.
Takaoka, A., Yanai, H., 2006. Interferon signalling network in innate defence. Cell Microbiol. 8 (6), 907–922.
Takeuchi, O., Akira, S., 2008. MDA5/RIG-I and virus recognition. Curr. Opin. Immunol. 20 (1), 17–22.
Triantafilou, K., Vakakis, E., Kar, S., Richer, E., Evans, G.L., Triantafilou, M., 2012a. Visualisation of direct interaction of MDA5 and the dsRNA replicative intermediate form of positive strand RNA viruses. J. Cell Sci. 125 (Pt 20), 4761–4769.
Vlotides, G., Sorensen, A.S., Kopp, F., Zitzmann, K., Cengic, N., Brand, S., Zachoval, R., Auernhammer, C.J., 2004. SOCS-1 and SOCS-3 inhibit IFN-alpha-induced expression of the antiviral proteins 2,5-OAS and MxA. Biochem. Biophys. Res. Commun. 320 (3), 1007–1014.
Yang, C.H., Murti, A., Pfeffer, S.R., Fan, M., Du, Z., Pfeffer, L.M., 2008. The role of TRAF2 binding to the type I interferon receptor in alternative NF kappaB activation and antiviral response. J. Biol. Chem. 283 (21), 14309–14316.
Yoneyama, M., Kikuchi, M., Natsukawa, T., Shinobu, N., Imaizumi, T., Miyagishi, M., Taira, K., Akira, S., Fujita, T., 2004. The RNA helicase RIG-I has an essential function in double-stranded RNA-induced innate antiviral responses. Nat. Immunol. 5 (7), 730–737.
Yoneyama, M., Suhara, W., Fukuhara, Y., Fukuda, M., Nishida, E., Fujita, T., 1998. Direct triggering of the type I interferon system by virus infection: activation of a transcription factor complex containing IRF-3 and CBP/p300. EMBO J. 17 (4), 1087–1095.
Zhao, Y., Valbuena, G., Walker, D.H., Gazi, M., Hidalgo, M., DeSousa, R., Oteo, J.A., Goez, Y., Brasier, A.R., 2016. Endothelial cell proteomic response to Rickettsia conorii infection reveals activation of the janus kinase (JAK)-Signal transducer and activator of transcription (STAT)-Interferon stimulated gene (ISG)15 pathway and reprogramming plasma membrane integrin/cadherin signaling. Mol. Cell. Proteomics 15 (1), 289–304.
Zhu, Z., Wang, G., Yang, F., Cao, W., Mao, R., Du, X., Zhang, X., Li, C., Li, D., Zhang, K., Shu, H., Liu, X., Zheng, H., 2016. Foot-and-Mouth disease virus viroporin 2B antagonizes RIG-I-mediated antiviral effects by inhibition of its protein expression. J. Virol. 90 (24), 11106–11121.